Available online at www.sciencedirect.com

SCIENCE DIRECT

Virology 341 (2005) 284 – 300

VIROLOGY

www.elsevier.com/locate/yviro

Bioluminescence imaging of vaccinia virus: Effects of interferon on viral replication and spread

Kathryn E. Luker[a], Martha Hutchens[b], Tracey Schultz[a], Andrew Pekosz[c], Gary D. Luker[a,d,*]

[a]Department of Radiology, University of Michigan Medical School, Ann Arbor, MI 48109-0648, USA
[b]Graduate Program in Immunology, University of Michigan Medical School, Ann Arbor, MI 48109-0648, USA
[c]Department of Molecular Microbiology, Department of Pathology and Immunology, Washington University School of Medicine, St. Louis, MO 63110, USA
[d]Department of Microbiology and Immunology, University of Michigan Medical School, Ann Arbor, MI 48109-0648, USA

Received 12 May 2005; returned to author for revision 23 June 2005; accepted 30 June 2005
Available online 10 August 2005

Abstract

Whole animal imaging allows viral replication and localization to be monitored in intact animals, which provides significant advantages for determining viral and host factors that determine pathogenesis. To investigate effects of interferons on spatial and temporal progression of vaccinia infection, we generated recombinant viruses that express firefly luciferase or a monomeric orange fluorescent protein. These viruses allow vaccinia infection to be monitored with bioluminescence or fluorescence imaging, respectively. The recombinant viruses were not attenuated in vitro or in vivo relative to a control WR virus. In cell culture, reporters could be detected readily by 4 h post-infection, showing that these viruses can be used as early markers of infection. The magnitude of firefly luciferase activity measured with bioluminescence imaging in vitro and in vivo correlated directly with increasing titers of vaccinia virus, validating imaging data as a marker of viral infection. Replication of vaccinia was significantly greater in mice lacking receptors for type I interferons (IFN I $R^{-/-}$) compared with wild-type mice, although both genotypes of mice developed focal infections in lungs and brain after intranasal inoculation. IFN I $R^{-/-}$ mice had greater dissemination of virus to liver and spleen than wild-type animals even when mortality occurred at the same time point after infection. Protective effects of type I interferons were mediated primarily through parenchymal cells rather than hematopoietic cells as analyzed by bone marrow transplant experiments. Collectively, our data define a new function for type I interferon signaling in systemic dissemination of vaccinia and validate these reporter viruses for studies of pathogenesis.

Keywords: Vaccinia; Bioluminescence imaging; Interferon

Smallpox was eradicated as a human disease before molecular tools were available to analyze the cellular and molecular effects of various viral proteins and the host immune response to infection. As a result, the complex interactions between virus and host immunity that determine pathogenesis of poxvirus infection remain incompletely defined. Because of the threat of smallpox as a potential agent of bioterrorism, there is renewed emphasis on developing new techniques and reagents to investigate viral and host determinants of disease in relevant animal models (Harrison et al., 2004). It is expected that identifying and characterizing specific viral and host mediators of pathogenesis will lead to new strategies for vaccination against poxvirus infection and novel targets for therapy. These are key areas of research because of the risk for complications associated with the existing smallpox vaccine (Wollenberg and Engler, 2004) and limitations of available drugs to treat infections with poxviruses (Ortiz et al., 2005).

Vaccinia virus was used as the vaccine to eradicate smallpox as a human disease, and vaccinia now is established as the model virus for poxvirus biology and disease (Harrison et al., 2004). Intranasal infection of mice with vaccinia reproduces spread of smallpox through the upper respiratory

* Corresponding author. Department of Radiology, University of Michigan Medical School, 1150 West Medical Center Drive, 9301 MSRB III, Ann Arbor, MI 48109-0648, USA.
E-mail address: gluker@umich.edu (G.D. Luker).

0042-6822/$ - see front matter © 2005 Elsevier Inc. All rights reserved.
doi:10.1016/j.virol.2005.06.049

tract, which is believed to be the typical route of infection (Breman and Henderson, 2002). Vaccinia replicates in the respiratory tract and lungs and then can disseminate systemically to visceral organs. Systemic infection may be cleared or progress to death, depending on factors such as viral inoculum, mouse age, and variations in immune response (Turner, 1967a; Williamson et al., 1990).

Interferons (IFN) are one of the key mediators of host innate immunity to vaccinia virus and other viruses. There are two major classes of IFNs produced in response to viral infection: type I and type II. Type I IFNs, which in mice and humans include multiple isotypes of IFN-α and a single isotype of IFN-β, are secreted by most cells in response to viral infection (Samuel, 1998). Production of type II IFN (IFN-γ) is restricted to activated $CD4^+$ and $CD8^+$ T lymphocytes, natural killer (NK) cells, and natural killer T (NKT) cells (Farrar and Schreiber, 1993; Fujii et al., 2002). Type I and II IFNs bind and signal through distinct heterodimeric receptors (IFN I R and IFN II R, respectively), each of which is expressed normally on all nucleated cells (Stark et al., 1998). In response to viral infection, specific isotypes of type I IFNs (IFN-β and IFN-α4) are secreted early in the host immune response. These IFNs bind to the type I IFN receptor and subsequently induce other subtypes of type I IFNs, as well as type II IFN, thereby establishing a positive feedback loop for amplifying anti-viral effects of both types of IFNs (Marie et al., 1998; Sato et al., 1998, 2000; Taniguchi and Takaoka, 2001).

Both type I and II IFN are important mediators of host immunity to vaccinia infection. Mice lacking receptors for type II IFN (IFN II $R^{-/-}$) are more susceptible to vaccinia infection than wild-type animals, and deletion of receptors for type I IFN (IFN I $R^{-/-}$) diminishes resistance to vaccinia to an even greater extent than IFN II $R^{-/-}$ mice (Huang et al., 1993; van den Broek et al., 1995). Combined deficiency of both type I and type II IFN receptors (IFN I/II $R^{-/-}$) produces an additive phenotype of susceptibility to vaccinia, as demonstrated by higher titers of virus in lungs after intranasal infection (van den Broek et al., 1995). Collectively, these previous studies emphasize the key functions of interferons in the immune response to vaccinia and indicate that type I interferon has a quantitatively greater impact than type II IFN on replication of vaccinia in vivo.

Vaccinia virus encodes a variety of proteins that inhibit IFN and its mediators, including soluble binding proteins for types I and II IFN and antagonists of the PKR pathway of anti-viral defense (reviewed in Katze et al., 2002). Viruses lacking these modulators of IFN are attenuated in vivo, further demonstrating the importance of IFN in host defense to vaccinia (Brandt and Jacobs, 2001; Sroller et al., 2001; Verardi et al., 2001). In cultured cells, the PKR antagonists E3L and K3L have been identified as key determinants of the host range for vaccinia (Langland and Jacobs, 2002). However, the extent to which IFN regulates dissemination of vaccinia to various organs and tissues in vivo has not been established.

Research by our laboratory and others demonstrates several significant advantages of investigating viral-host pathogenesis with imaging (Cook and Griffin, 2003; Luker et al., 2002). Spatial and temporal progression of infection can be quantified in the same animals, identifying animal-to-animal variations in viral replication and dissemination and host immunity. Imaging greatly increases data obtained about viral pathogenesis in living mice compared with other global assays of disease progression, such as weight loss or external signs of disease. Imaging data also allow relative amounts of viral replication in various anatomic sites to be quantified over time. These data otherwise require sacrifice of animals at multiple time points for determinations of viral titers in excised organs and tissues. Importantly, imaging techniques can identify unexpected sites or patterns of viral infection that could be missed if organs are not collected or if entire organs are analyzed for viral titers (Luker et al., 2003).

To exploit the advantages of imaging for studies of vaccinia pathogenesis, we generated a recombinant vaccinia virus that expresses firefly luciferase (FL) to enable bioluminescence imaging (BLI) of vaccinia virus infection in living mice. We also engineered a recombinant vaccinia virus that expresses a monomeric orange fluorescent protein (mKO) to facilitate analyses of infected tissues by microscopy. Unlike many reporter viruses for vaccinia, these recombinant viruses were constructed without deleting any viral genes (Blasco and Moss, 1991). This strategy allows our reporter viruses to reproduce replication and dissemination of wild-type virus in cultured cells and mice. We used these recombinant viruses to investigate to what extent innate immunity mediated through interferons regulates replication and dissemination of vaccinia. Our research demonstrated that type I interferons limit replication of vaccinia virus and that the protective effects of type I IFN are mediated primarily through parenchymal rather than hematopoietic cells. We also determined that type I IFN regulates dissemination of vaccinia virus to specific tissues following intranasal inoculation.

Results

Bioluminescent and fluorescent reporter vaccinia viruses for imaging

Recombinant vaccinia viruses typically are constructed by replacing a viral gene, such as thymidine kinase, with a heterologous protein. While this strategy facilitates selection of recombinant viruses, replacement of thymidine kinase is known to attenuate vaccinia virus in mice (Buller et al., 1985). Even disruption of a potential open reading frame in the viral genome may attenuate vaccinia and limit the use of the recombinant virus for studies of pathogenesis (Coupar et al., 2000).

We used an alternative strategy based on repair of a mutant virus to engineer vaccinia viruses with reporter genes for imaging. The system is based on a WR strain of vaccinia that has a mutation in *vp37*, a gene for a protein in the outer viral membrane that is essential for efficient cell-to-cell spread. The recombination vector repairs *vp37* and inserts a foreign gene driven by a strong synthetic vaccinia virus p7.5 early/late promoter (Blasco and Moss, 1995). This system enabled us to produce vaccinia viruses that express either firefly luciferase (Vac-FL) or a monomeric orange fluorescent protein (Vac-mKO) for bioluminescence imaging or identification of infected cells, respectively (Karasawa et al., 2004). We also constructed a virus that repaired the *vp37* gene without insertion of a reporter gene as a marker rescue virus. The marker rescue virus differs from wild-type WR only by insertion of the p 7.5 early/late promoter into the genome.

To validate the virulence of the reporter viruses used in this study, we quantified growth of Vac-FL and Vac-mKO relative to the marker rescue virus and wild-type WR in a multi-step growth assay. Vero cells were infected with various viruses at an MOI of 0.1, and viral titers were quantified for 3 days post-infection. The kinetics of viral replication did not differ among the four viruses, demonstrating that the reporter viruses were not attenuated in vitro (Fig. 1). Sizes of plaques were comparable among the recombinant viruses and repaired virus, while the parental mutant virus did not form plaques within 3 days (data not shown).

Because attenuation of vaccinia viruses only may be apparent in vivo, we compared Vac-FL with the marker rescue WR vaccinia virus in an intranasal model of infection in mice. WT mice were infected with 1×10^6 pfu of Vac-FL or marker rescue WR virus. Bioluminescence imaging was performed daily on mice infected with Vac-FL, and weights of animals in both groups were measured on each day post-infection. Infection with Vac-FL or the marker rescue virus had comparable weight loss over time, and mice were euthanized on day 7 post-infection after losing 30% of initial body weight (Fig. 2A). We quantified viral titers in lung, brain, and spleen from mice on days 3 and 7 post-infection (Figs. 2B and C). These organs were selected as sites of local infection (lung) and disseminated disease (brain and spleen), respectively. Titers of Vac-FL and marker rescue virus did not differ in these organs on either day. Collectively, these data indicate that insertion of FL or the bioluminescence imaging protocol did not attenuate vaccinia or its pathogenicity in mice.

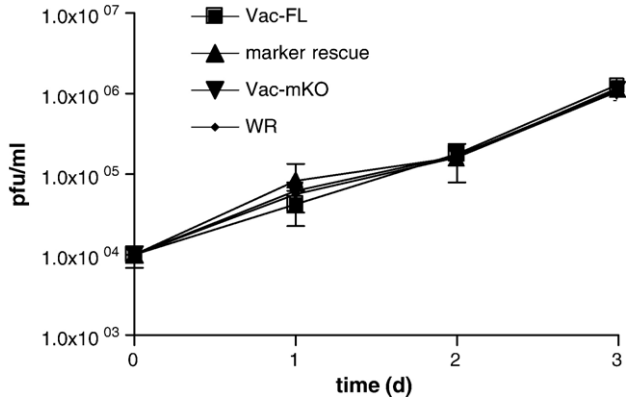

Fig. 1. Replication of Vac-FL and Vac-mKO in vitro. Vero cells were infected with Vac-FL, Vac-mKO, marker rescue virus, or wild-type WR at an MOI of 0.1. Cells were harvested every 24 h after infection for determinations of viral titers by plaque assay. Each data point is the mean of three independent determinations. Error bars represent SEM. Data are representative of two independent experiments.

Having established that expression of FL did not attenuate the recombinant virus, we determined the extent to which bioluminescence imaging of luciferase activity could be used to quantify replication of Vac-FL in vivo. WT mice were infected intranasally with 1×10^6 pfu Vac-FL, and mice were euthanized immediately after bioluminescence imaging on day 7 post-infection. Animals were dissected rapidly to verify sites of FL activity identified by in vivo imaging. Excised organs were imaged within 5 min after euthanizing each mouse to quantify photon flux, and plaque assays then were performed on these same organs. Relative to in vivo imaging, ex vivo imaging of bioluminescence in excised organs has potential limitations, including changes in cell metabolism and oxygenation, loss of perfusion, and alterations in intracellular concentration of luciferin. In part, these limitations can be overcome by maintaining a consistent time interval between euthanasia of mice and imaging. We observed a direct correlation between relative values for photon flux and viral titers in lung, brain, liver, and spleen (Fig. 3). These data demonstrate that bioluminescence imaging data for FL can be used as a reporter for relative amounts of Vac-FL in various anatomic sites.

Detection of reporter genes in cultured cells

We determined the kinetics of FL activity following infection of Vero cells with Vac-FL at an MOI of 5. Luciferase activity from Vac-FL was quantified by imaging at various times through 24 h post-infection, and these same samples also were analyzed for viral titers. Bioluminescence was slightly above background levels at 1 h post-infection (Fig. 4A). FL activity continued to increase at subsequent time points, reaching a level that was 4 logs above uninfected cells by 24 h. Viral titers decreased initially, corresponding to entry of virus into cells and the start of replication. Titers of Vac-FL at 24 h were approximately 15-fold greater than the input inoculum of virus. These data show that the synthetic early/late promoter in Vac-FL allows rapid production of the FL imaging reporter and a large dynamic range for quantifying vaccinia infection.

We further characterized the FL reporter by determining the limits of bioluminescence imaging for detecting Vac-FL in cultured cells. Monolayers of Vero cells in 6-well plates were infected with Vac-FL at various pfu, and photon flux

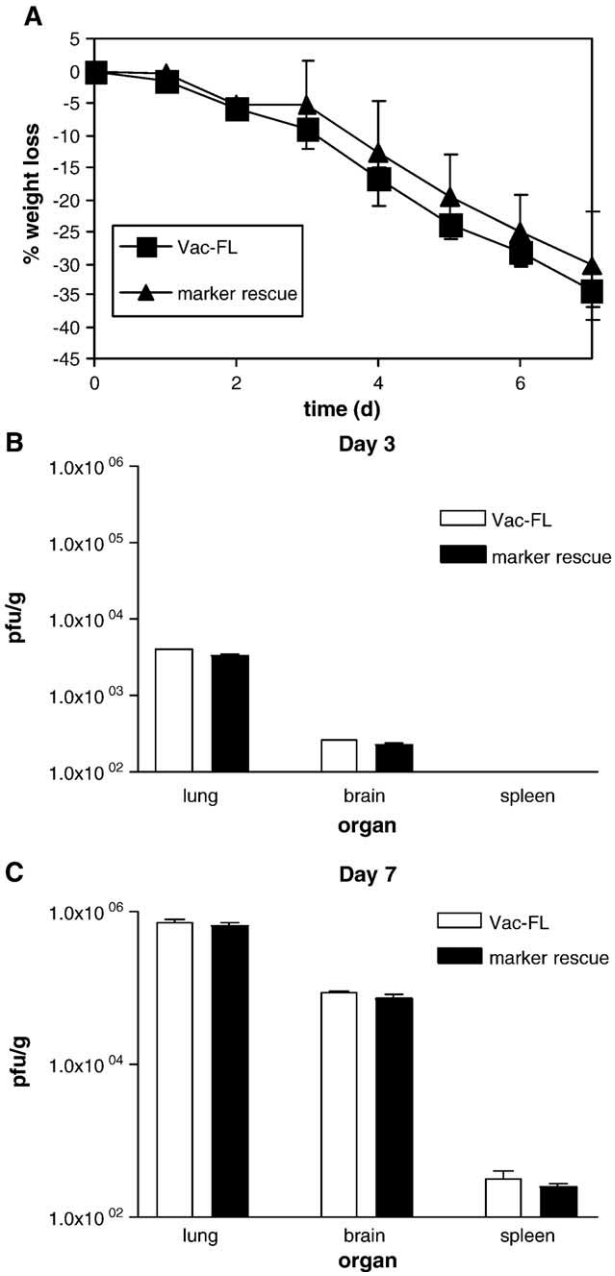

Fig. 2. Pathogenesis and replication of Vac-FL in mice. 129 Ev/Sv mice (WT) were infected with 1×10^6 pfu of Vac-FL or marker rescue WR by intranasal (i.n.) inoculation ($n = 8$ mice per virus). (A) Mice were weighed daily to monitor overall progression of disease. Data are presented as mean ± SEM percent loss of initial weight. (B) Viral titers in lung, brain, and spleen at days 3 and 7 post-infection were quantified by plaque assay ($n = 4$ mice per time point). Data are shown as mean ± SEM of vaccinia virus pfu/g tissue. The lower limits of detection for the plaque assay were 30 pfu/g tissue.

from FL was quantified 12 h post-infection. FL activity was detectable above background levels using an input of 30 pfu per well, although viral replication would have occurred in the interval between infection and the measurement of bioluminescence. The lower limits for detecting Vac-FL in vitro and in vivo with bioluminescence imaging will vary based on factors including numbers of virions per unit volume of cells or tissues and overlying materials that absorb light. Nevertheless, this result provides a guideline for the sensitivity of bioluminescence imaging for detecting Vac-FL in cultured cells.

We also assayed the time course of expression of mKO by Vac-FL over time as described for Vac-FL. After infection at an MOI of 5, flow cytometry showed that approximately 17% of cells expressed mKO after 1 h. The percentage of orange cells increased to approximately 40% by 4–12 h post-infection and increased to more than 70% at 24 h post-infection (Fig. 4B). While the percentages of orange cells increased over time, the mean fluorescence intensity from the population of orange cells was similar in samples acquired between 1 and 24 h post-infection. By comparison, titers of Vac-mKO decreased immediately post-

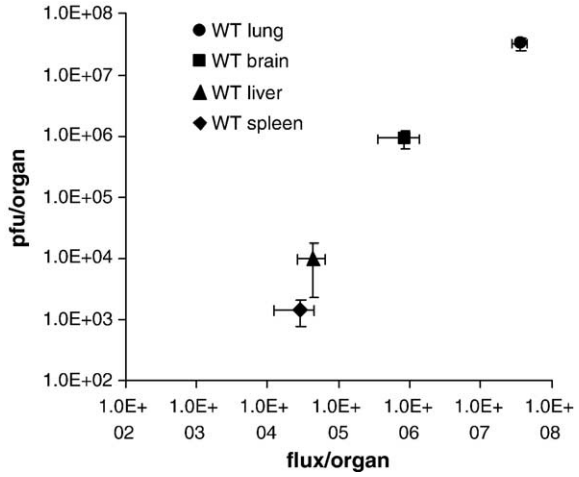

Fig. 3. Correlation of luciferase activity with viral titers. WT mice ($n = 5$) were infected with 1×10^6 pfu of Vac-FL i.n. Bioluminescence imaging of infected mice was performed on day 7 post-infection, and mice were euthanized immediately after imaging. Firefly luciferase activity in excised lung, brain, liver, and spleen was quantified by imaging. Viral titers in excised organs were quantified by plaque assay. Mean values ± SEM for photon flux and pfu per organ are shown on the x and y axes, respectively. Lower limits of detection for photon flux and plaque assay are at the origin of each axis.

infection and increased by approximately 13-fold at 24 h. Both the kinetics of mKO expression after infection and changes in titers of Vac-mKO over time were comparable to those quantified with Vac-FL. Overall, these data demonstrate that both FL and mKO can be detected at early times after infection, thereby providing reporters for monitoring vaccinia infection by bioluminescence and fluorescence imaging.

Bioluminescence imaging of Vac-FL in WT, IFN I $R^{-/-}$, and IFN I/II $R^{-/-}$ mice

We used IFN I $R^{-/-}$ and IFN I/II $R^{-/-}$ mice to determine to what extent types I and II IFN alter replication and dissemination of vaccinia virus in vivo. Mice were infected with 1×10^5 pfu of Vac-FL by intranasal inoculation. Bioluminescence imaging was performed daily on all mice to monitor progression of infection, using the distribution of amount of photons emitted by FL to analyze sites of infection and relative amounts of reporter virus (Luker et al., 2002). Weights of infected mice also were measured daily to assess overall health of infected mice (Fig. 5A).

Bioluminescence imaging over the course of infection showed progressively increasing amounts of FL activity at the local site of viral inoculation in the nose (Figs. 5B, C). By day 3 post-infection, bioluminescence could be detected in the chest of IFN I $R^{-/-}$ and IFN I/II $R^{-/-}$ mice, corresponding to sites of Vac-FL infection in trachea and lungs. Systemic dissemination of Vac-FL to abdominal organs including liver, spleen, and inguinal lymph nodes was observed in these same genotypes of mice by day 5. Bioluminescence in both chest and abdomen increased over time in both IFN I $R^{-/-}$ and IFN I/II $R^{-/-}$ mice. IFN I/II $R^{-/-}$ animals developed more pronounced dissemination to sites in the abdomen than IFN I $R^{-/-}$ mice, although Vac-FL disseminated to the same organs and tissues in both genotypes of mice. IFN I/II $R^{-/-}$ mice were euthanized because of weight loss 5 days after infection, while IFN I $R^{-/-}$ animals survived until day 6. By comparison, bioluminescence in WT mice increased over time in the local site of infection in the nose. Low levels of FL from infection in the lungs could be detected in the chest of WT mice on days 4–6 post-infection. Luciferase activity from Vac-FL FL decreased rapidly after day 6. Only minimal FL activity from Vac-FL could be identified in abdominal organs of WT mice at any time point, and all WT mice survived the infection.

We quantified FL produced by Vac-FL using region-of-interest (ROI) analysis of head, chest, and abdomen of infected mice. These data are presented as the daily amount of FL activity in each site, and cumulative amounts of viral replication for the first 5 days of the experiment are summarized by AUC analysis of photon flux over time (Figs. 5C and D). AUC data end at day 5 because that is the time when IFN I/II $R^{-/-}$ mice were euthanized because of severe illness. Photon flux data for the head ROI showed a progressive increase in bioluminescence from Vac-FL in each genotype of mouse. AUC analysis showed that photon flux in heads of IFN I $R^{-/-}$ and IFN I/II $R^{-/-}$ mice did not differ significantly, while intact IFN signaling pathways in WT mice decreased amounts of Vac-FL at the local site of infection ($P < 0.05$).

Differences between WT and mice with deletion of IFN receptors became substantially greater in the chest and abdominal regions. Vac-FL in the chest ROI of IFN I $R^{-/-}$ and IFN I/II $R^{-/-}$ mice increased rapidly between day 2 and 5 post-infection, while only low levels of FL were quantified in this anatomic location on WT mice. In the abdomen, FL activity was quantitatively greater in IFN I/II $R^{-/-}$ mice relative to IFN I $R^{-/-}$ animals, showing that that combined effects of type I and II interferons limit are more effective than type I interferon alone in limiting systemic dissemination of vaccinia. Intact signaling through both type I and II IFN receptors prevented detectable dissemination of Vac-FL to abdominal organs in WT mice.

By AUC analysis, FL activity from Vac-FL in chest did not differ between IFN I $R^{-/-}$ and IFN I/II $R^{-/-}$ mice, but both of these genotypes were significantly greater than WT mice over the initial 5 days after infection ($P < 0.001$). Differences between IFN I $R^{-/-}$ and IFN I/II $R^{-/-}$ mice in spread of Vac-FL to abdominal organs were significant over this same time period ($P < 0.05$), and both genotypes of mutant mice had greater amounts of Vac-FL in the abdomen than WT animals. Collectively, these data confirm previous research showing that IFN

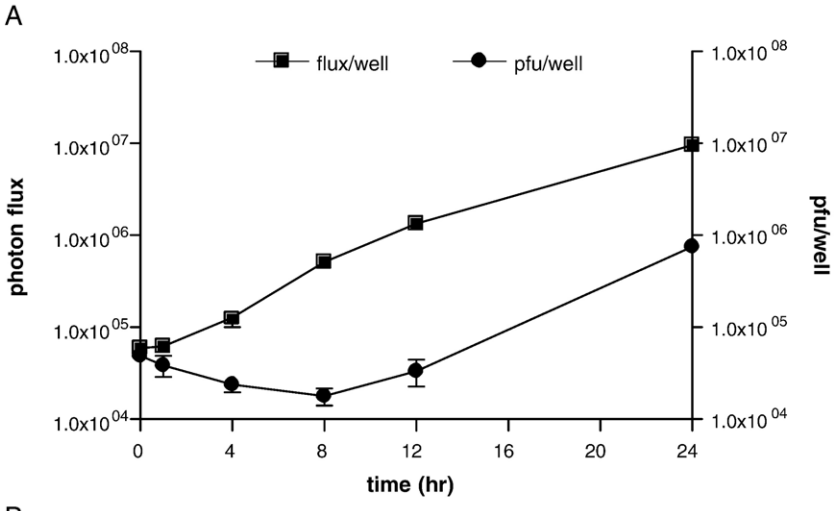

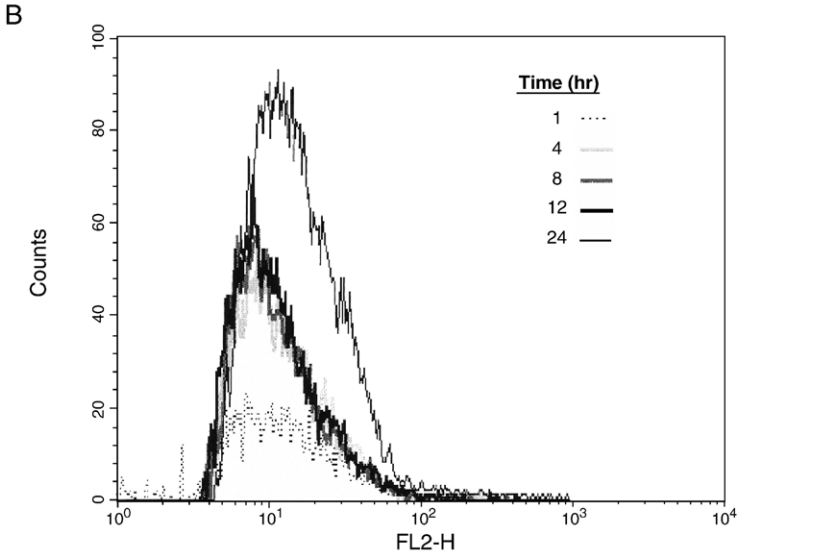

Time post-infection (hr)	Mean fluorescence intensity	% orange cells	Titer x 10^5 pfu/ml ± sem
0	2.6	0	4.1±0.8
1	16.0	17.4	2.8±0.9
4	14.8	37.2	1.8±0.3
8	13.6	38.6	1.7±0.1
12	13.7	42.1	2.0±0.2
24	20.4	74.3	52.5±3.6

Fig. 4. Kinetics of reporter gene expression from Vac-FL and Vac-mKO. Vero cells were infected with Vac-FL (A) or Vac-mKO (B) at an MOI of 5. Luciferase activity or fluorescence in infected cells was quantified at various times post-infection by bioluminescence imaging (A) or flow cytometry (B), respectively (n = 3 for Vac-FL and n = 2 for Vac-mKO per time point). Viral titers also were quantified in infected cells at these same time points. Values are mean ± SEM for photon flux (A). Histograms from infected samples are shown after subtraction of the histogram for uninfected cells (B). Numeric values for mean fluorescence intensity, percent orange cells, and pfu/ml at each time point are tabulated. Data for Vac-FL are representative of 2 independent experiments, while results for Vac-mKO are from a single experiment.

signaling limits replication of vaccinia virus in lungs (van den Broek et al., 1995). Type I IFN confers most IFN-mediated host immunity to vaccinia virus, although combined functions of types I and II IFN further restrict systemic spread of vaccinia. In addition, our results show that IFN signaling regulates dissemination of vaccinia virus to intraabdominal organs including liver and spleen. Because of the predominant function of type I IFN receptors in vaccinia infection, we focused our subsequent studies on IFN I $R^{-/-}$ and WT mice.

Vac-FL produces focal infections in lungs and brain

Bioluminescence imaging in living mice showed focal areas of increased luciferase activity in lungs rather than a uniform distribution of Vac-FL. This pattern of infection was detected in WT and IFN I $R^{-/-}$ mice. To verify this finding, we rapidly removed lungs of infected mice immediately after in vivo imaging at various times between 1 and 7 days post-infection and imaged luciferase activity in excised lungs. This strategy exploits the fact that bioluminescence from luciferase can be detected in tissues after euthanizing animals. Bioluminescence could not be detected in excised lungs 1 day after intranasal infection (data not shown). On subsequent days, specimens from WT and IFN I $R^{-/-}$ mice both showed focal areas of luciferase activity from Vac-FL in lungs (Figs. 6A and B). The amount of luciferase activity increased over time and spread to adjacent lung tissue. However, the multifocal pattern of Vac-FL persisted on all subsequent days, which is consistent with aspiration of Vac-FL administered intranasally.

We analyzed microscopic sites of vaccinia infection in lungs by infecting WT and IFN I $R^{-/-}$ mice with 1×10^6 or

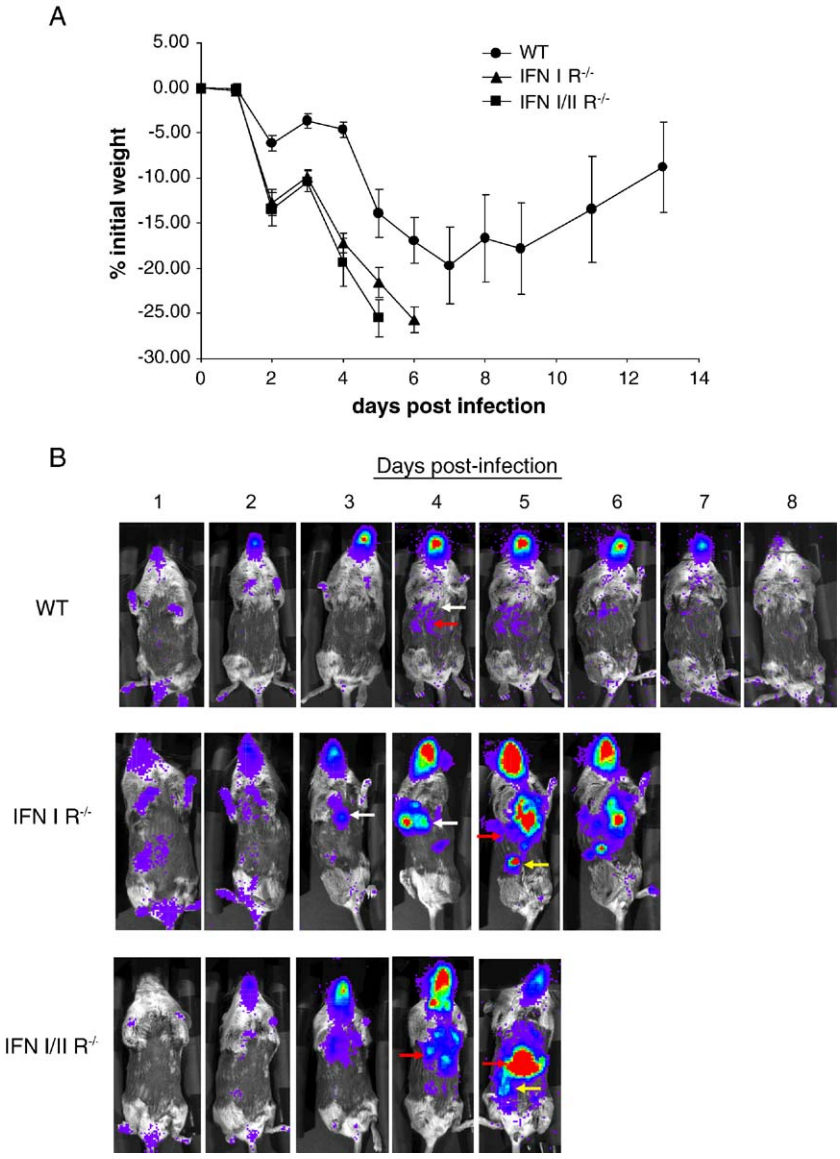

Fig. 5. Bioluminescence imaging of Vac-FL in WT, IFN I $R^{-/-}$, and IFN I/II $R^{-/-}$ mice. Mice ($n = 5$ per genotype) were infected with 1×10^6 pfu of Vac-FL i.n. (A) Weights of animals are expressed as mean values ± SEM for percent initial weight for each genotype of mouse. Weights for a genotype end on the graph when animals were euthanized because of disease severity. (B) Bioluminescence imaging of mice infected with Vac-FL. Luciferase activity is depicted with a pseudocolor scale using red as the highest and blue as the lowest levels of photon flux, respectively. The pseudocolor scale is set for all images with the minimum value at background noise of the instrument and a uniform level of maximum photon flux. White arrow, lung; red arrow, liver; yellow arrow, lymph node. (C) Luciferase activity from Vac-FL was quantified by ROI analysis of the head, chest, and abdomen. Data represent mean values for photon flux ± SEM. (D) AUC analyses of photon flux for each genotype of mouse over the first 5 days after infection. Error bars represent SEM. $^*P < 0.05$; $^{**}P < 0.001$.

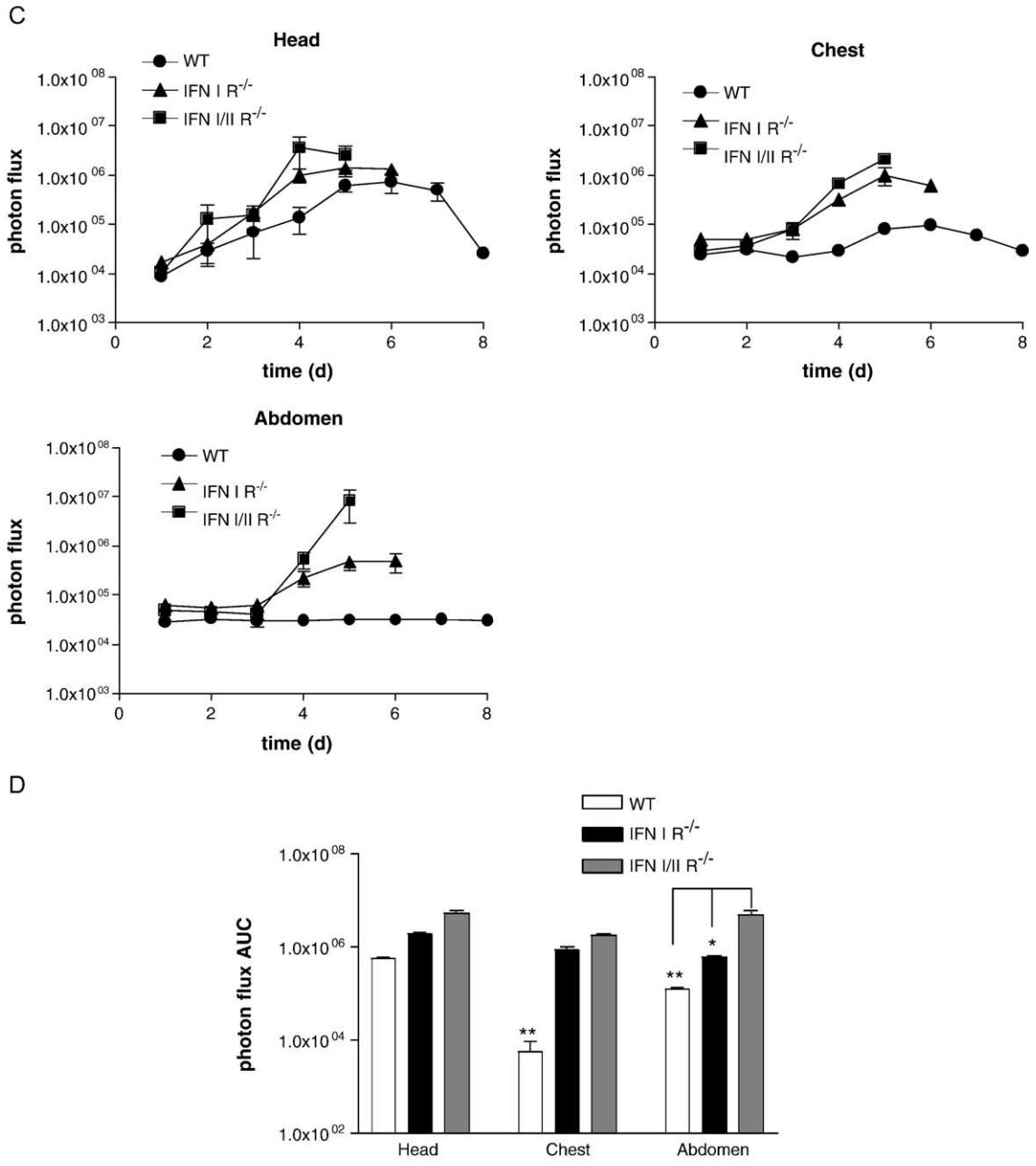

Fig. 5 (*continued*).

1×10^5 pfu, respectively, of Vac-mKO. Infected lungs were removed daily between 1 and 4 days after intranasal infection. Fluorescence from Vac-mKO infection initially could be detected on day 2 following infection. Sites of viral infection localized predominantly to bronchioles in the lung, as evidenced by fluorescence microscopy and confirmed by hematoxylin and eosin staining of adjacent sections (Figs. 6C–E). An inflammatory infiltrate composed primarily of mononuclear cells was identified adjacent to an infected bronchiole. Similar to bioluminescence data, Vac-mKO produced a multifocal pattern of infection with areas of uninfected lung positioned between discontiguous sites of infection. Collectively, these data show that intranasal infection with vaccinia produces multiple foci of infection in lungs and suggest that the infection may begin in bronchiolar epithelium.

Ex vivo imaging of brains removed from infected WT and IFN I $R^{-/-}$ mice repeatedly demonstrated that luciferase activity was restricted to a focal area in the anterior, inferior aspect of the frontal lobes (Fig. 7A). This localized area of bioluminescence in the brain was not detectable in living mice because of the high levels of Vac-FL in the nasopharynx and sinuses of mice following intranasal inoculation. To confirm this pattern of vaccinia infection in the brain, we used intranasal inoculation of Vac-mKO. Fluorescence microscopy of tissue sections from brain

showed focal orange fluorescence in the same distribution identified by bioluminescence imaging (Fig. 7B). Focal infection of the frontal lobes following intranasal inoculation of vaccinia potentially could be due to an inability of virus to infect other parts of the brain. We investigated this possibility by infecting IFN I $R^{-/-}$ mice with 1×10^4 pfu Vac-FL by direct intracranial injection of virus into the left parietal lobe. Following direct injection of virus, Vac-FL spread to other parts of the brain within 2 days, as monitored by in vivo and ex vivo bioluminescence imaging (Figs. 7C and D). These data show that focal infection of the anterior, inferior aspects of the frontal lobes after intranasal infection is not caused by resistance of other parts of the brain to vaccinia infection.

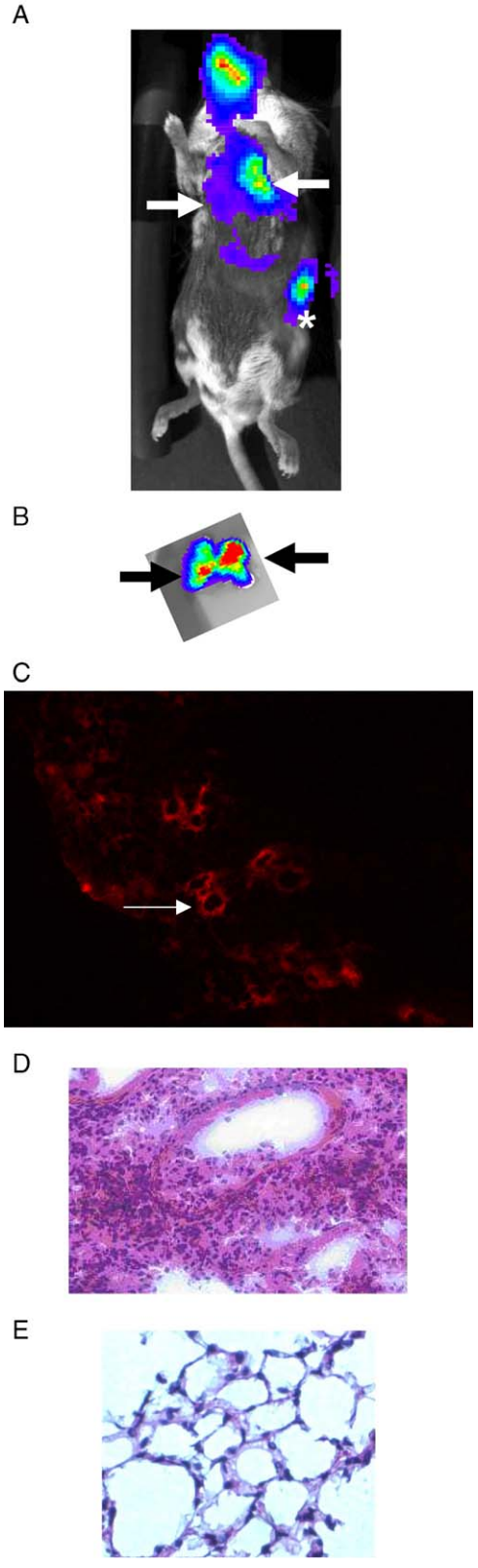

Fig. 6. Focal vaccinia infection in lungs. IFN I $R^{-/-}$ mice were infected with 1×10^5 pfu Vac-FL or Vac-mKO i.n. (A) Bioluminescence image obtained 4 days post-infection shows focal areas of increased luciferase activity in lungs (arrows). Infection also is present in the spleen (asterisk). (B) Ex vivo image of lungs demonstrates corresponding focal areas of Vac-FL infection. (C) Fluorescence microscopy (4× objective) shows Vac-mKO localized primarily to bronchioles. The arrow shows a bronchiole that was examined at higher magnification (40× objective) in panel D. (D) Hematoxylin and eosin staining shows a predominantly mononuclear cell infiltrate adjacent to the bronchiole of a WT mouse infected with Vac-FL. (E) A lung specimen from an uninfected mouse is shown for comparison.

Vaccinia infection is limited to a greater extent by type I IFN receptors on parenchymal cells relative to hematopoietic cells

Studies in WT and IFN I $R^{-/-}$ mice showed that signaling through type I IFN receptors was essential for limiting local replication of vaccinia and subsequent systemic dissemination. To determine the extent to which type I IFN limits vaccinia infection through effects on hematopoietic cells versus parenchymal cells in organs and tissues, we established chimeric mice by transferring bone marrow between WT and IFN I $R^{-/-}$ mice. We also transplanted bone marrow from WT to WT animals as a control. Mice were infected with 1×10^5 pfu Vac-FL i.n. 6 weeks after bone marrow transplantation. As additional controls, age-matched WT and IFN I $R^{-/-}$ mice that had not undergone bone marrow transplantation were infected with the same inoculum of Vac-FL. Viral replication and dissemination were monitored daily with bioluminescence imaging, and data for photon flux were analyzed by AUC analysis for the 7 days that all animals survived.

AUC analysis of photon flux in the head, which is dominated by Vac-FL in the intranasal site of infection, showed that IFN I $R^{-/-}$ mice had significantly higher luciferase activity from Vac-FL than the other groups for days 1 to 7 post-infection ($P < 0.05$; Fig. 8A). Comparable amounts of bioluminescence were quantified in heads of IFN I $R^{-/-}$ mice transplanted with WT bone marrow, IFN I $R^{-/-}$ to WT transplants, and WT to WT mice. WT mice had the lowest calculated value for head AUC ($P < 0.05$). Differences among groups of mice were larger for AUC data calculated from images of the chest and abdomen. In the chest, AUC for photon flux was highest in the WT to IFN I $R^{-/-}$ transplant and IFN I $R^{-/-}$ mice, while AUC in the

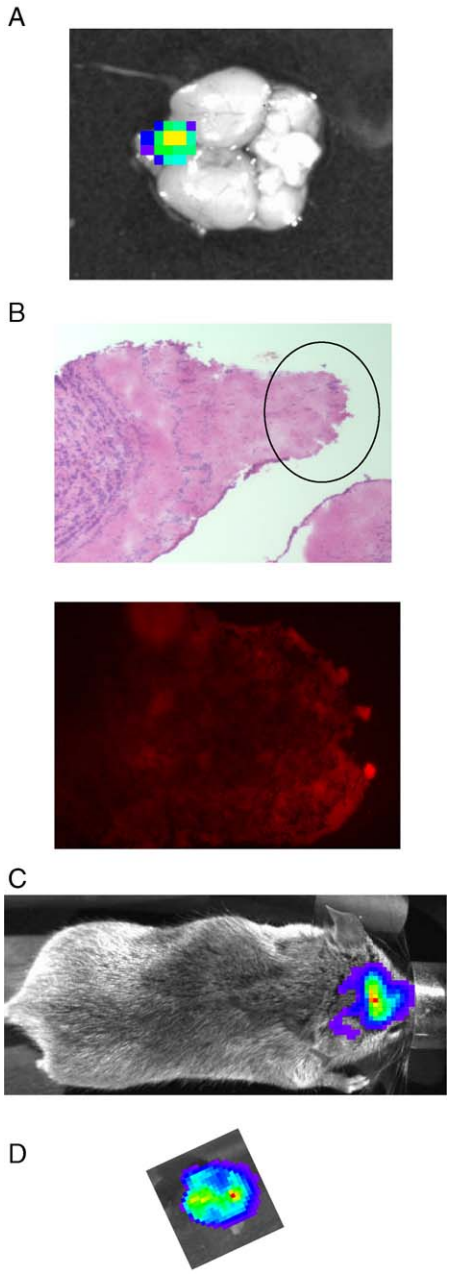

Fig. 7. Focal vaccinia infection in brain. (A) Ex vivo bioluminescent image of the ventral surface of the brain shows focal bioluminescence (arrow) in an IFN I $R^{-/-}$ 7 days post-infection with 1×10^6 pfu Vac-FL i.n. (B) Hematoxylin and eosin staining of a section obtained from the ventral surface of the frontal lobe (4× objective). The circled area in panel B was examined at higher magnification (20× objective) for Vac-mKO by fluorescence microscopy on an immediately adjacent section. (C) Bioluminescence image of IFN I $R^{-/-}$ mouse injected intracranially with 1×10^4 pfu Vacl-FL shows dissemination of virus throughout the brain on day 2 post-infection. (D) Ex vivo bioluminescent image of the brain of the same mouse removed immediately after in vivo imaging.

abdomen was greatest for IFN I $R^{-/-}$ mice ($P < 0.05$). AUC data in chest and abdomen for WT to IFN I $R^{-/-}$ mice and untransplanted IFN I $R^{-/-}$ animals were significantly greater than all other mice ($P < 0.001$). IFN I $R^{-/-}$ to WT transplant mice were more susceptible to vaccinia infection than WT mice as quantified by AUC of photon flux in the chest and abdomen ($P < 0.01$). AUC values in these sites also were significantly greater in WT to WT transplant mice as compared with WT animals ($P < 0.01$).

The number of days that groups of mice survived after intranasal infection corresponded with AUC data for photon flux from Vac-FL. IFN I $R^{-/-}$ mice with WT bone marrow and IFN I $R^{-/-}$ mice were euthanized on day 7 post-infection because of weight loss of approximately 30% (Fig. 8B). IFN I $R^{-/-}$ to WT transplant mice and WT to WT mice survived through day 9. WT mice lost approximately 12% of body weight by day 7 post-infection, but these animals all regained weight and survived. Collectively, these data show that protective effects of type I IFN against vaccinia virus are mediated to a quantitatively greater extent through parenchymal tissues as compared with hematopoietic cells.

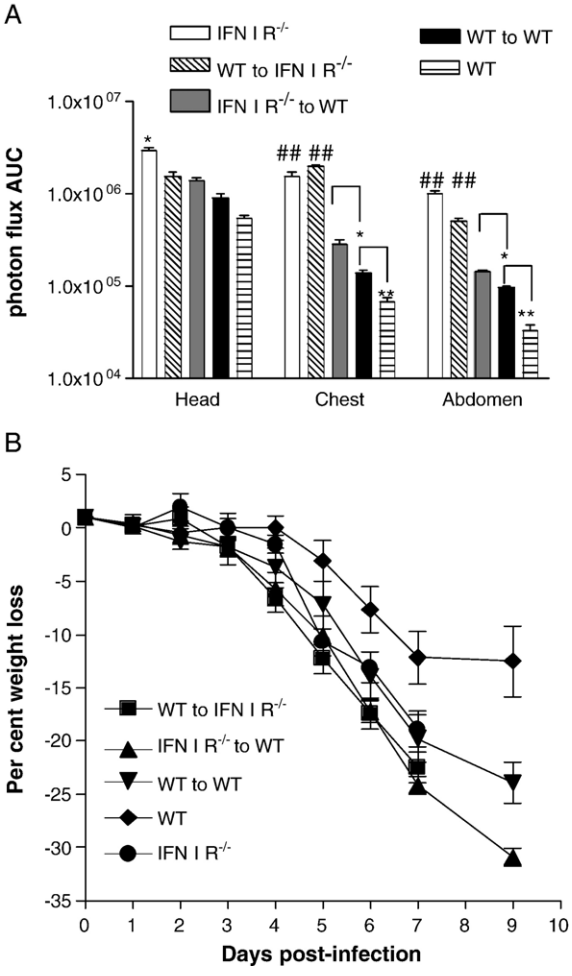

Fig. 8. Vac-FL infection in WT and IFN I $R^{-/-}$ bone marrow transplant mice. WT, WT bone marrow to WT, WT bone marrow to IFN I $R^{-/-}$, IFN I $R^{-/-}$ bone marrow to WT, and IFN I $R^{-/-}$ mice ($n = 5–6$ per condition) were infected with 1×10^5 pfu Vac-FL i.n. Bioluminescence imaging was performed daily, and replication and spread of Vac-FL were quantified by ROI analysis. AUC data for days 1–7 post-infection are presented for defined ROIs in head, chest, and abdomen. Error bars represent SEM. *$P < 0.05$; **$P < 0.01$; #$P < 0.001$.

Lethal infection with Vac-FL produces comparable amounts of virus in lungs and brain of WT and IFN I $R^{-/-}$ mice

Data from in vivo experiments showed that signaling through type I IFN receptors is an essential component of host immunity to vaccinia virus. When infected with the same input pfu, Vac-FL replicated to a greater extent in IFN I $R^{-/-}$ mice than WT animals. Notably, systemic dissemination of virus to anatomic sites including liver, spleen, and lymph nodes was significantly more extensive in IFN I $R^{-/-}$ mice. Potentially, this result could be caused by a function of type I IFN to limit dissemination of vaccinia to these organs and tissues independent of amounts of viral replication. Alternatively, it was possible that type I IFN signaling produced a relative barrier to systemic dissemination of vaccinia, and comparable spread of virus beyond the lungs would occur in WT mice infected with a lethal inoculum of V-FL.

To distinguish between these possible effects of signaling through type I IFN receptors, we infected IFN I $R^{-/-}$ and WT mice with amounts of virus that produced comparable progression to lethality in both groups. Intranasal infection of WT and IFN I $R^{-/-}$ mice with 1×10^6 and 9×10^4 pfu of Vac-FL, respectively, produced comparable weight loss in each genotype of mouse (Fig. 9A). Both groups of animals were euthanized because of disease severity at 7 days after infection.

Bioluminescence imaging showed that luciferase activity quantified in head regions of WT mice was greater than IFN I $R^{-/-}$ animals, consistent with the greater input inoculum of Vac-FL (Figs. 9B and E). Luciferase activity from Vac-FL in the chest was comparable at all times after infection, and total AUC for photon flux in the chest did not differ significantly between the two genotypes (Figs. 9C and E). By comparison, spread of Vac-FL to abdominal organs and tissues was significantly greater in IFN I $R^{-/-}$ mice relative to WT animals ($P < 0.01$), even when viral replication in the chest and the overall weight loss associated with infection were the same (Figs. 9D and E).

We used ex vivo imaging of excised organs and quantification of viral titers on day 7 post-infection to validate data from in vivo imaging. Luciferase activity and viral titers in spleen and liver of IFN I $R^{-/-}$ mice were approximately 10-fold greater than those quantified in WT animals ($P < 0.001$; Figs. 9F and G). Amounts of virus in blood were slightly higher in WT mice, although these differences were not statistically significant. These data for viral titers in blood suggest that lack of receptors for type IFN did not limit dissemination of virus from lungs under conditions in which overall progression of disease was comparable (Fig. 9G). By comparison, bioluminescence and titers of Vac-FL in lung and brain did not differ significantly on day 7 post-infection, which is the time when both genotypes of mice were euthanized because of the severity of disease (Figs. 9F and G). These data imply that viral infection and associated pathology in lungs and/or brain may be key determinants of lethality, independent of dissemination of virus to other organs and tissues.

Discussion

In vivo studies of poxviruses in the integrated physiology of a living animal are essential to understanding the cellular and molecular determinants of pathogenesis. Conventional studies of viral-host pathogenesis are based on infecting large numbers of animals and euthanizing subsets of animals at various time points to collect organs to determine localization and titers of virus. This approach requires large numbers of animals and precludes direct correlations between viral replication and the outcome of disease in individual animals. In addition, anatomic localization of infection within an organ and/or dissemination of virus to unexpected sites may be missed by harvesting selected organs and titering total amounts of virus. Previous studies by our laboratory and others have demonstrated that imaging can be used to investigate viral infection in mouse models and identify new aspects of pathogenesis in vivo. To enable imaging studies of vaccinia virus, we have developed new recombinant viruses with fluorescent or bioluminescent reporter proteins. A key feature of these recombinant vaccinia viruses is that they are not attenuated in vitro or in vivo, making these viruses important new tools for analyzing host–pathogen interactions in vaccinia infection.

Vac-FL and Vac-mKO allow complementary approaches for imaging vaccinia infection. Vac-FL exploits the sensitivity of firefly luciferase to allow sensitive detection of virus in vitro and in vivo. Luciferase activity from Vac-FL is directly proportional to titers of vaccinia virus, allowing relative differences in amounts of virus in various anatomic sites to be quantified with bioluminescence imaging. This reporter virus builds upon previous work with recombinant vaccinia viruses that express firefly luciferase. Rodriguez et al. constructed a virus with firefly luciferase replacing the thymidine kinase gene in vaccinia and showed that as few as 10^{-6} pfu per cell could be detected in homogenates of cells 18 h after infection (Rodriguez et al., 1988). This virus also provided sensitive detection of vaccinia in homogenates of infected

Fig. 9. Type I IFN signaling affects dissemination of Vac-FL to liver and spleen without affecting overall survival. WT and IFN I $R^{-/-}$ mice ($n = 5$ each) were infected i.n. with 1×10^6 and 9×10^4 pfu of Vac-FL, respectively, to produce comparable rates of overall infection as determined by weight loss and mortality. (A) Data for animal weights are presented as mean values ± SEM for percent initial weight on each day post-infection. (B–D) Photon flux quantified from bioluminescence imaging data on days 1–7 post-infection in head (B), chest (C), and abdomen (D). (E) AUC data summarizing photon flux in head, chest, and abdomen ROIs for each genotype of mouse. (F) Photon flux and (G) viral titers in excised organs. 30 pfu/g tissue is the lower limits of detection for titers. *$P < 0.01$; **$P < 0.001$.

tissues from mice. The current Vac-FL has the advantage of retaining full virulence in vivo, and it likely provides greater sensitivity for detecting viruses because the firefly luciferase in Vac-FL has improved expression in mammalian cells. Previous studies with transgenic mice that express firefly luciferase also demonstrate a high correlation among presence of luciferase, bioluminescence produced in vivo, and luciferase activity in homogenates of excised tissues (Zhang

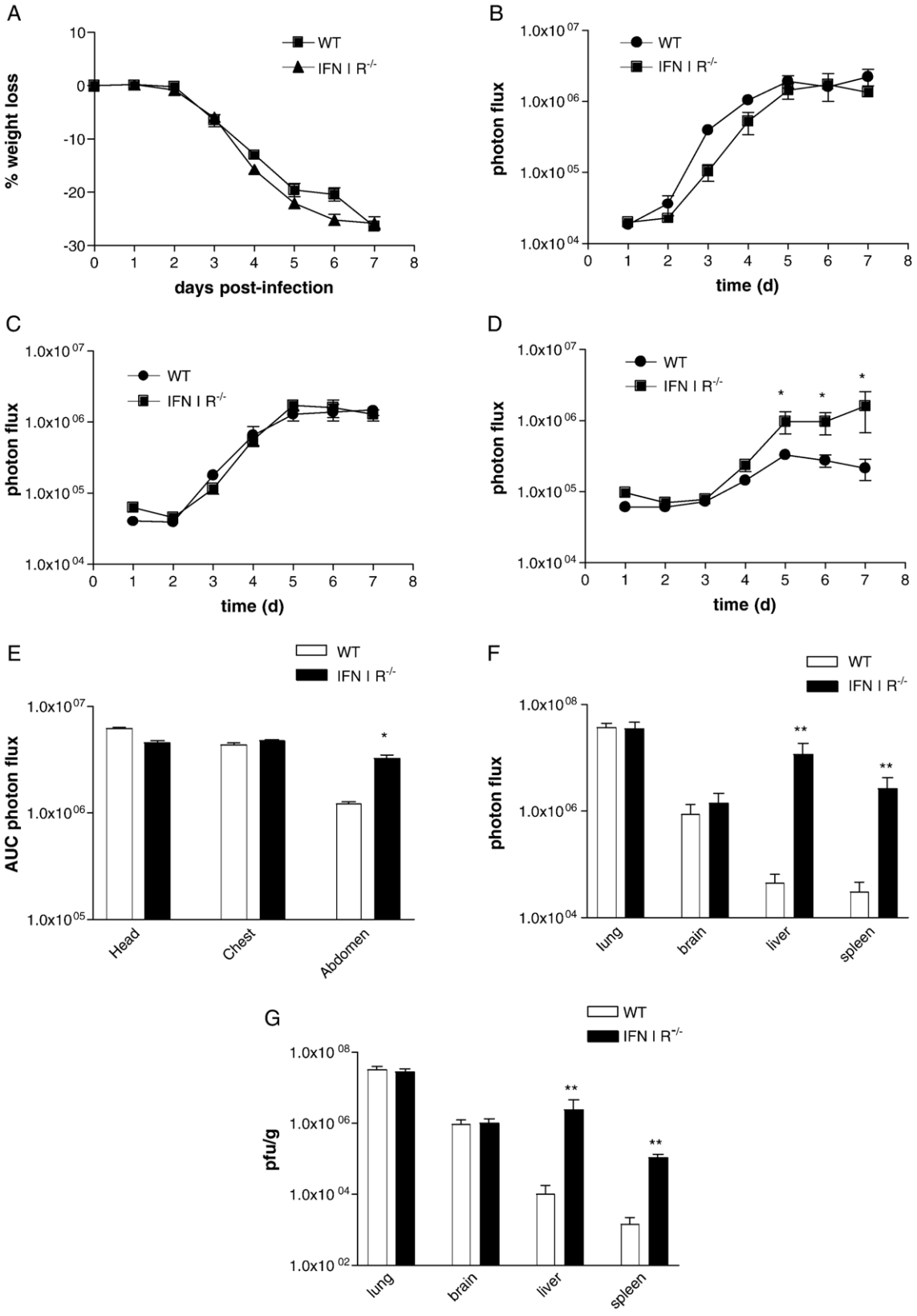

et al., 2001). Collectively, these data support the use of luciferase activity produced by Vac-FL as a sensitive reporter of vaccinia virus in living mice and for in vitro assays.

Vac-mKO enables facile detection of anatomic sites infected with vaccinia using fluorescence imaging. Using an orange fluorescent protein shifts fluorescence from the reporter away from autofluorescence that can limit detection of the commonly used GFP reporter in tissues. The relatively high quantum yield of fluorescence from mKO also enhances detection of Vac-mKO in tissue specimens (Karasawa et al., 2004). While we have used Vac-mKO to detect vaccinia in tissue sections, the favorable properties of this fluorescent reporter should enhance detection of Vac-mKO for future studies of the immune response to vaccinia with intravital two-photon microscopy. In addition, it should be feasible to construct a reporter virus that maintains the virulence of wild-type WR while expressing both FL and a fluorescent protein either as separate proteins or as a fusion protein. We currently are developing this type of recombinant vaccinia virus to enable macroscopic and microscopic imaging of infection in the same animal.

We have used these reporter viruses to investigate effects of IFN on pathogenesis of vaccinia virus in mice. In particular, we focused on functions of type I IFN in host resistance to vaccinia. Type I IFN confers an approximately 10-fold reduction in the amount of virus necessary to produce lethal infection in mice. These data confirm the established functions of type I IFN in limiting replication of vaccinia and other viruses. However, we have determined that type I IFN also affects dissemination of virus from the respiratory system to systemic sites. Even when infected with amounts of virus that produce comparable progression of overall disease, IFN I $R^{-/-}$ mice have significantly higher amounts of virus in liver and spleen than WT animals at the time of death. Because total amounts of vaccinia virus in blood are similar between both genotypes of mice, these data suggest that type I IFN affects the intrinsic susceptibility of cells within liver and spleen to infection with vaccinia. However, additional studies with isolated cultures of various types of primary cells from these organs will be needed to separate effects of dissemination from intrinsic susceptibility of cells to vaccinia. Our imaging data with IFN I/II $R^{-/-}$ mice also showed similar spread of Vac-FL to liver and spleen after intranasal infection, although levels of bioluminescence in these organs were higher in IFN I/II $R^{-/-}$ animals relative to IFN I $R^{-/-}$ animals. Collectively, these data demonstrate a key function of type I IFN for dissemination of vaccinia virus to liver and spleen.

Our results with vaccinia viruses are consistent with other recent studies that demonstrate a function of IFN pathways in dissemination of viruses. For example, coxsackievirus 3B replicates selectively in the heart of wild-type mice without causing lethality. IFN I $R^{-/-}$ mice infected with coxsackievirus 3B have comparable titers of virus in the heart, but greatly enhanced spread of virus to the liver causes death in these mutant mice (Wessely et al., 2001). Ryman et al. demonstrated that Sindbis virus disseminated to macrophage-dendritic cells in various organs in IFN I $R^{-/-}$ mice, while these sites were not infected with Sindbis in WT mice (Ryman et al., 2000). Similarly, we have shown that absence of type I IFN signaling permits HERPES simplex virus type I to spread from a mucosal site of infection to liver and spleen (Luker et al., 2003).

Despite the function of type I IFN to limit spread of vaccinia virus to systemic organs such as liver and spleen, our data suggest that vaccinia infection in lungs and/or brain may be more important determinants of mortality in mice. When the input inoculum of vaccinia virus was adjusted to produce comparable overall progression of disease as monitored by weight loss and time to death, WT and IFN I $R^{-/-}$ mice had equal amounts of vaccinia virus in lung and brain, as quantified by bioluminescence and viral titer. Although these data do not allow us to distinguish the relative contributions of viral replication versus immune-mediated damage, our results imply that lethality is due to pathology in the lungs and/or brain.

The combination of in vivo imaging and fluorescence microscopy shows that vaccinia produces focal infection in lungs and brain of infected mice. Focal infection in lungs could be anticipated based on patterns of aspiration of liquids into dependent portions of anesthetized animals (Franquet et al., 2000). However, localization of vaccinia to the anterior, inferior aspects of the frontal lobes of the brain after intranasal inoculation was unexpected. This site of vaccinia infection in the brain is adjacent to the olfactory bulbs, suggesting that the mechanism of neuroinvasion was direct spread of virus from the nasal mucosa via the olfactory system. The potential for vaccinia to enter the brain by direct cell-to-cell spread rather than hematogenous dissemination is supported by previous research with vaccinia and cowpox (Martinez et al., 2000; Turner, 1967b). By histology, cowpox antigens were detected in perineural fibroblasts adjacent to the olfactory nerve, and viral antigens extended to the leptomeninges surrounding the olfactory tract. A variety of other viruses, including influenza A and vesicular stomatitis virus, also appear to enter the brain directly along the olfactory nerves (Aronsson et al., 2003; Plakhov et al., 1995). By comparison, Sindbis virus and Venezuelan equine encephalitis virus are believed to spread from blood to the nasal neuroepithelium before entering the brain (Charles et al., 1995; Cook and Griffin, 2003). A more detailed study of the kinetics and microscopic localization of vaccinia in the nervous system will be necessary to establish definitively that spread through the olfactory route is a mechanism of neuroinvasion by vaccinia.

We used a bone marrow transplant approach to establish the extent to which signaling through receptors for type I IFN in parenchymal cells contributes to the innate immune response to vaccinia infection. IFN I $R^{-/-}$ mice transplanted with WT bone marrow were significantly more susceptible

to Vac-FL than WT mice that received bone marrow from IFN I $R^{-/-}$ mice. However, type I IFN signaling in both the parenchymal and hematopoietic compartments was necessary for mice to have normal immunity to vaccinia. Our results are consistent with similar studies showing that innate immune responses activated by toll receptors in both parenchymal tissues and hematopoietic cells are essential for normal responses to bacterial and viral pathogens (Sato and Iwasaki, 2004; Schilling et al., 2003). Collectively, these data demonstrate the critical function of parenchymal cells in the IFN-mediated immune response to vaccinia infection and emphasize the interrelated functions of IFN in hematopoietic and parenchymal cells.

Interestingly, the bone marrow transplant experiments also showed that WT to WT transplant mice were more susceptible to vaccinia infection than WT animals that did not undergo bone marrow transplantation. Potentially, this result may be due to residual damage to parenchymal tissues and endothelium as a result of irradiation used to prepare for bone marrow transplantation (Giaid et al., 2003). However, previous studies suggest that irradiation may alter immune control of pathogens. Following total body gamma-irradiation, mice become susceptible to pulmonary infection with cytomegalovirus because of defective responses of T lymphocytes (Reddehase et al., 1985). Mice that have undergone total body irradiation and bone marrow transplantation also are more susceptible to infection with *Pseudomonas aeruginosa* after intratracheal inoculation of the organism. Greater replication of *Pseudomonas aeruginosa* was associated with impaired phagocytosis of alveolar macrophages, reduced levels of specific cytokines, and lower levels of selected integrins (Ojielo et al., 2003). These data suggest that specific immune defects caused by the procedure of bone marrow transplantation impair the host response to vaccinia infection. This susceptibility is relevant to development of improved vaccines against smallpox and their possible use in the general population. Mechanisms that cause the increased susceptibility of bone marrow transplant recipients to vaccinia investigation are under investigation in our laboratory.

While the current study demonstrates numerous advantages of imaging for investigating vaccinia pathogenesis in vivo, it also shows limitations of the present technology. Current instruments for bioluminescence imaging provide two-dimensional images. This limitation may be overcome in part by obtaining images from several different projections to localize sites of bioluminescence in three-dimensional space. However, the focal infection of the brain was obscured by high amounts of Vac-FL in the nasopharynx and paranasal sinuses of mice following intranasal inoculation of virus. We anticipate that this type of problem with bioluminescence imaging will be substantially improved as three-dimensional imaging systems become available commercially (Wang et al., 2004).

In summary, we have established two new reporter viruses for imaging vaccinia virus pathogenesis. Importantly, the method used to engineer these viruses does not attenuate vaccinia in vitro and in vivo, and these viruses can be engineered further to delete specific target genes of interest. The imaging reporters validated in this study enabled us to detect unexpected patterns of vaccinia infection in vivo and establish effects of type I IFN on viral dissemination. Beyond the role of imaging demonstrated in the current study, other research has shown that BLI and magnetic resonance imaging (MRI) also can be used to monitor responses of defined populations of immune cells in vivo (Cao et al., 2004; Dubey et al., 2003; Edinger et al., 2003; Kircher et al., 2003). We anticipate that combined imaging studies of vaccinia infection and the host immune response to the virus will enhance greatly in vivo studies of pathogenesis and facilitate testing of candidate vaccines and anti-viral compounds in vivo.

Materials and methods

Cells

Vero cells were cultured in DMEM medium with 10% heat-inactivated fetal bovine serum, 1% L-glutamine, and 0.1% penicillin–streptomycin in a 5% CO_2 incubator at 37 °C.

Recombinant viruses

Recombinant viruses were constructed in vRB12, a WR strain of vaccinia with deletion of the F13L gene for *vp37* (Blasco and Moss, 1991). The RB21 transfer vector is designed to insert a foreign gene and restore a functional *vp37* protein following homologous recombination with vRB12 (Blasco and Moss, 1995). To prepare the transfer plasmid for firefly luciferase (FL), we digested FL from pGL3 Basic (Promega) with *Xba*I and blunted with Klenow. pGL3 basic then was digested with *Nhe*I and ligated to the *Nhe*I and *Sma*I sites in pRB21. Monomeric orange fluorescent protein (mKO; Medical and Biological Laboratories, Ltd.) was digested with *Eco*RI and *Hin*dIII, respectively, and ligated to the corresponding sites in pRB21.

2×10^5 Vero cells were plated in 35 mm dishes and infected 1 day later with vRB12 at an MOI of 1. One hour post-infection, cells were transfected with pRB21 containing FL or mKO, respectively. Transfection with pRB21 alone was used to rescue *vp37* and produce a control virus containing the early/late promoter in pRB21 but lacking a reporter gene. Transfections were performed with Lipofectamine (Invitrogen) or Fugene 6 (Roche) according to the manufacturer's instructions. Cells were harvested 2 days post-infection by scraping, and three cycles of freeze-thaw were used to release viruses. Recombinant viruses were prepared by infecting Vero cells as described previously (Blasco and Moss, 1995). Recombinant viruses containing

FL (Vac-FL) were selected based on restoration of normal plaque formation 2 days post-infection, while recombinants with mKO (Vac-mKO) were identified by fluorescence microscopy. Viruses were plaque-purified three times before preparing viral stocks (Earl et al., 1998).

Mouse strains

All mice were in a pure 129 Ev/Sv background (referred to as wild type). Immunocompetent wild-type (WT) mice were purchased from Taconic (Germantown). Mice deficient in type I IFN receptors (IFN I $R^{-/-}$) or type I and II IFN receptors (IFN I/II $R^{-/-}$) were bred at the University of Michigan (Muller et al., 1994). Experiments were performed with adult mice. Mice were 6–10 weeks old for all studies except for the bone marrow transplant experiment, in which mice were 7 weeks old at the time of transplantation and 13 weeks old when infected. There were no effects of age on susceptibility to vaccinia infection among the various cohorts of adult mice. Both male and female mice were used in all experiments except that only males were used for bone marrow transplantation. Numbers of male and female mice in various experimental groups were matched, although we did not observe a difference between sexes of mice in susceptibility to vaccinia infection.

Viral replication in cells

Vero cells were plated at 100,000 cells per well in 6-well plates for multi-step growth of various viruses at an MOI of 0.1. Cells in triplicate wells were harvested for plaque assays at various time points after infection by scraping cells into culture medium. To quantify bioluminescence from Vac-FL over time, Vero cells were plated at 400,000 cells per well in 35 mm dishes and infected with Vac-FL at an MOI of 5. Bioluminescence from FL was quantified by adding 150 μg/ml D-luciferin (Promega) to culture medium 10 min before imaging dishes of cells with a cryogenically cooled CCD camera system (IVIS, Xenogen Corporation). Triplicate samples were imaged at various time points after infection. Viral titers in infected cells were analyzed by plaque assay. Bioluminescence was quantified by manually defined region-of-interest (ROI) analysis, and data were expressed as photon flux. The relationship between Vac-FL pfu and bioluminescence was performed by infecting Vero cells (400,000 cells per well in 6-well plates) with various amounts of Vac-FL between 30 and 1×10^5 pfu. Bioluminescence was quantified by imaging as described above.

Fluorescence from Vac-mKO over time was measured by infecting 35 mm dishes of Vero cells (400,000 cells per dish) with Vac-mKO at an MOI of 5. Duplicate wells were trypsinized to release cells for analysis of fluorescence by flow cytometry at various times post-infection as shown in the figure (FACScalibur, BD Biosciences). Mean fluorescence intensity was quantified at each time point. Data for percent orange cells were analyzed by subtracting the histogram for uninfected cells from the histograms obtained from samples at various time points post-infection. Duplicate wells infected in parallel were harvested for determinations of viral titers by plaque assay.

Virus titration

Cells harvested from experiments in tissue culture were lysed by three cycles of freezing and thawing prior to plaque assays. Organs and tissues excised from mice at various time points after infection were manually homogenized as described previously (Luker et al., 2003). Liver, spleen, brain, and lungs were homogenized in 3 ml of medium, while lymph nodes and trachea were collected in 0.5 ml of medium. Whole blood was obtained by cardiac puncture and diluted with 1 ml of culture medium. Samples were frozen and thawed three times prior to plaque assays.

Viral titers in cells and organs were assayed by serial dilution on Vero cells plated at 400,000 cells per well in 6-well plates. Plaque assays were performed according to a standard protocol (Earl et al., 1998), and plaques were counted 3 days after infection.

Mouse infection

All animal procedures were approved by the University of Michigan University Committee on Use and Care of Animals. For intranasal infection with vaccinia viruses, mice were anesthetized with subcutaneous injection of ketamine (100 mg/kg) and xylazine (15 mg/kg). Mice were inoculated intranasally with 20 μl of virus diluted in DMEM. Anesthetized mice were shaved with clippers to decrease absorption and scattering of light for bioluminescence imaging. Weights of animals were determined immediately prior to infection and then daily throughout the course of each infection.

Bone marrow transplantation

Bone marrow was harvested from femora and tibiae of donor mice and resuspended at a concentration of 2×10^7 cells per milliliter in sterile PBS. Recipient mice were irradiated with a total of 11 Gy divided into two equal doses separated by 3 h. Mice received 4×10^6 bone marrow cells suspended in 200 μl PBS injected via a 30 g needle into the retroorbital venous plexus. Mice were housed in autoclaved cages and received autoclaved food and water after transplantation. Experiments were performed 6 weeks after transplantation of bone marrow. Control mice that received PBS alone died approximately 10 days after irradiation.

Microscopic analysis of organs

Selected organs were excised from mice and frozen in OCT compound. Lungs were inflated with 1 ml of a solution

containing 1% low melting point agarose in phosphate-buffered saline immediately before removal. 6 μm frozen sections were prepared from various tissues and fixed in 4% paraformaldehyde. For fluorescence microscopy of VacmKO, sections were incubated in 10 mM glycine for 10 min to quench background fluorescence. Frozen sections adjacent to the corresponding fluorescence section were stained with hematoxylin and eosin.

Bioluminescence imaging

Bioluminescence imaging was performed with a cryogenically cooled CCD camera (IVIS) as described previously (Luker et al., 2002). ROIs corresponding to the head, chest, and abdomen of infected mice were used to quantify bioluminescence as photon flux. For some experiments, mice were euthanized immediately after imaging, and selected organs were dissected rapidly and imaged ex vivo within 5 min to quantify bioluminescence on the imaging system (Luker et al., 2003). Bioluminescence from these organs was quantified by ROI analysis, and background bioluminescence was measured from the same size ROI positioned adjacent to each organ. Background subtracted photon flux was calculated for each organ. These same organs were then analyzed for viral titers by plaque assay.

Statistics

Pairs of data points were analyzed by *t* test for statistically significant differences ($P < 0.05$). Statistics for area-under-the-curve analyses were performed with commercially available software (Graphpad, Prism).

Acknowledgments

The authors thank Bernard Moss for providing vRB12 and pRB21 and reviewing the manuscript. The authors also thank Myria Petrou and Bradley Foerster for help with animal experiments. Research was supported in part by NIH grant P50-CA093990-04. Support for imaging experiments was provided by NIH R24CA083099 for the University of Michigan Small Animal Imaging Resource.

References

Aronsson, F., Robertson, B., Ljunggren, H., Kristensson, K., 2003. Invasion and persistence of the neuroadapted influenza virus A/WSN/33 in the mouse olfactory system. Viral. Immunol. 16 (3), 415–423.

Blasco, R., Moss, B., 1991. Extracellular vaccinia virus formation and cell-to-cell virus transmission are prevented by deletion of the gene encoding the 37,000-Dalton outer envelope protein. J. Virol. 65 (11), 5910–5920.

Blasco, R., Moss, B., 1995. Selection of recombinant vaccinia viruses on the basis of plaque formation. Gene 158 (2), 157–162.

Brandt, T., Jacobs, B., 2001. Both carboxy- and amino-terminal domains of the vaccinia virus interferon resistance gene, E3L, are required for pathogenesis in a mouse model. J. Virol. 75 (2), 850–856.

Breman, J., Henderson, D., 2002. Diagnosis and management of smallpox. N. Engl. J. Med. 346 (17), 1300–1308.

Buller, R., Smith, G., Cremer, K., Notkins, A., Moss, B., 1985. Decreased virulence of recombinant vaccinia virus expression vectors is associated with a thymidine kinase-negative phenotype. Nature 317, 813–815.

Cao, Y., Wagers, A., Beilhack, A., Dusich, J., Bachman, M., Negrin, R., Weissman, I., Contag, C., 2004. Shifting foci of hematopoiesis during reconstitution from single stem cells. Proc. Natl. Acad. Sci. U.S.A. 101 (1), 221–226.

Charles, P., Walters, E., Margolis, F., Johnston, R., 1995. Mechanism of neuroinvasion of Venezuelan equine encephalitis virus in the mouse. Virology 208 (2), 662–671.

Cook, S., Griffin, D., 2003. Luciferase imaging of a neurotropic viral infection in intact animals. J. Virol. 77 (9), 5333–5338.

Coupar, B., Oke, P., Andrew, M., 2000. Insertion sites for recombinant vaccinia virus construction: effects on expression of a foreign protein. J. Gen. Virol. 81, 431–439.

Dubey, P., Su, H., Adonai, N., Du, S., Rosato, A., Braun, J., Gambhir, S., Witte, O., 2003. Quantitative imaging of the T cell antitumor response by positron-emission tomography. Proc. Natl. Acad. Sci. U.S.A. 100 (3), 1232–1237.

Earl, P., Cooper, N., Wyatt, L., Moss, B., 1998. Preparation of cell cultures and vaccinia virus stocks. In: Ausubel, F.M., Brent, R., Kingston, R.E., Moore, D.D., Seidman, J.G., Smith, J.A., Struhl, K. (Eds.), Current Protocols in Molecular Biology. John Wiley and Sons, Inc., pp. 16.16.1–16.16.11.

Edinger, M., Cao, Y., Verneris, M., Bachman, M., Contag, C., Negrin, R., 2003. Revealing lymphoma growth and the efficacy of immune cell therapies using in vivo bioluminescence imaging. Blood 101 (2), 640–648.

Farrar, M., Schreiber, R., 1993. The molecular cell biology of interferon-gamma and its receptor. Annu. Rev. Immunol. 11, 571–611.

Franquet, T., Gimenez, A., Roson, N., Torrubia, S., Sabate, J., Perez, C., 2000. Aspiration diseases: findings, pitfalls, and differential diagnosis. Radiographics 20 (3), 673–685.

Fujii, S., Shimizu, K., Kronenberg, M., Steinman, R., 2002. Prolonged IFN-gamma-producing NKT response induced with alpha-galactosylceramide-loaded DCs. Nat. Immunol. 3, 867–874.

Giaid, A., Lehnert, S., Chehayeb, B., Chehayeb, D., Kaplan, I., Shenouda, G., 2003. Inducible nitric oxide synthase and nitrotyrosine in mice with radiation-induced lung damage. Am. J. Clin. Oncol. 26 (4), e67–e72.

Harrison, S., Alberts, B., Ehrenfeld, E., Enquist, L., Fineberg, H., Mcknight, S., Moss, B., O'Donnell, M., Ploegh, H., Schmid, S., Walter, K., Theriot, J., 2004. Discovery of antivirals against smallpox. Proc. Natl. Acad. Sci. U.S.A. 101 (31), 11178–11192.

Huang, H., Hendriks, W., Althage, A., Hemmi, S., Bluethmann, H., Kamijo, R., Vilcek, J., Zinkernagel, R., Aguet, M., 1993. Immune response in mice that lack the interferon-gamma receptor. Science 259 (5102), 1742–1745.

Karasawa, S., Araki, T., Nagai, T., Mizuno, H., Miyawaki, A., 2004. Cyan-emitting and orange-emitting fluorescent proteins as a donor/acceptor pair for fluorescence resonance energy transfer. Biochem. J. 381 (Pt. 1), 307–312.

Katze, M., Yupeng, H., Gale, M., 2002. Viruses and interferon: a fight for supremacy. Nat. Rev., Immunol. 2, 675–687.

Kircher, M., Allport, J., Graves, E., Love, V., Josephson, L., Lichtman, A., Weissleder, R., 2003. In vivo high resolution three-dimensional imaging of antigen-specific cytotoxic T-lymphocyte trafficking to tumors. Cancer Res. 63 (20), 6838–6846.

Langland, J., Jacobs, B., 2002. The role of the PKR-inhibitory genes, E3L and K3L, in determining vaccinia virus host range. Virology 299 (1), 133–141.

Luker, G., Bardill, J., Prior, J., Pica, C., Piwnica-Worms, D., Leib, D., 2002.

Noninvasive bioluminescence imaging of herpes simplex virus type 1 infection and therapy in living mice. J. Virol. 76 (23), 12149–12161.

Luker, G., Prior, J., Song, J., Pica, C., Leib, D., 2003. Bioluminescence imaging reveals systemic dissemination of HSV-1 in the absence of interferon receptors. J. Virol. 77, 11082–11093.

Marie, I., Durbin, J., Levy, D., 1998. Differential viral induction of distinct interferon-alpha genes by positive feedback through interferon regulatory factor-7. EMBO J. 17, 6660–6669.

Martinez, M., Bray, M., Huggins, J., 2000. A mouse model of aerosol-transmitted orthopoxviral disease: morphology of experimental aerosol-transmitted orthopoxviral disease in a cowpox virus-BALB/c mouse system. Arch. Pathol. Lab. Med. 124 (3), 362–377.

Muller, U., Steinhoff, L., Reis, S., Hemmi, S., Pavlovic, J., Zinkernagel, R., Aguet, M., 1994. Functional role of type I and type II interferons in antiviral defense. Science 264, 1918–1921.

Ojielo, C., Cooke, K., Mancuso, P., Standiford, T., Olkiewicz, K., Clouthier, S., Corrion, L., Ballinger, M., Towes, G., Paine, R.r., Moore, B., 2003. Defective phagocytosis and clearance of *Pseudomonas aeruginosa* in the lung following bone marrow transplantation. J. Immunol. 171 (8), 4416–4424.

Ortiz, A., Justo, P., Sanz, A., Merlero, R., Caramelo, C., Guerrero, M., Strutz, F., Muller, G., Barat, a., Egido, J., 2005. Tubular cell apoptosis and cidofovir-induced acute renal failure. Antivir. Ther. 10 (1), 185–190.

Plakhov, I., Arlund, E., Aoki, C., Reiss, C., 1995. The earliest events in vesicular stomatitis virus infection of the murine olfactory neuroepithelium and entry of the central nervous system. Virology 209 (1), 257–262.

Reddehase, M., Weiland, F., Munch, K., Jonjic, S., Luske, A., Koszinowski, U., 1985. Interstitial murine cytomegalovirus pneumonia after irradiation: characterization of cells that limit viral replication during established infection of the lungs. J. Virol. 55 (2), 264–273.

Rodriguez, J., Rodriguez, D., Rodriguez, J., McGowan, E., Esteban, M., 1988. Expression of the firefly luciferase gene in vaccinia virus: a highly sensitive gene marker to follow virus dissemination in tissues of infected animals. Proc. Natl. Acad. Sci. U.S.A. 85 (5), 1667–1671.

Ryman, K., Klimstra, W., Nguyen, K., Biron, C., Johnston, R., 2000. Alpha/beta interferon protects adult mice from fatal Sindbis virus infection and is an important determinant of cell and tissue tropism. J. Virol. 74 (7), 3366–3378.

Samuel, C., 1998. Reoviruses and the interferon system. Curr. Top. Microbiol. Immunol. 223, 125–145.

Sato, A., Iwasaki, A., 2004. Induction of antiviral immunity requires Toll-like receptor signaling in both stromal and dendritic cell compartments. Proc. Natl. Acad. Sci. U.S.A. 101 (46), 16274–16279.

Sato, M., Hata, N., Asagiri, M., Nakaya, T., Taniguchi, T., Tanaka, N., 1998. Positive feedback regulation of type I IFN genes by the IFN-inducible transcription factor IRF-7. FEBS Lett. 425, 112–116.

Sato, M., Suemori, H., Hata, M., Asagiri, K., Ogasawara, K., Nakao, K., Nakaya, T., Katsuki, S., Noguchi, S., Tanaka, N., Taniguchi, T., 2000. Distinct and essential roles of transcription factors IRF-3 and IRF-7 in response to viruses for IFN-alpha/beta gene induction. Immunity 13, 539–548.

Schilling, J., Martin, S., Hung, C., Lorenz, R., Hultgren, S., 2003. Toll-like receptor 4 on stromal and hematopoietic cells mediates innate resistance to uropathogenic *Escherichia coli*. Proc. Natl. Acad. Sci. U.S.A. 100 (7), 4203–4208.

Sroller, V., Ludvikova, V., Maresova, L., Hainz, P., Nemeckova, S., 2001. Effect of IFN-receptor gene deletion on vaccinia-virus virulence. Arch. Virol. 146, 239–249.

Stark, G., Kerr, I., Williams, B., Silverman, R., Schreiber, R., 1998. How cells respond to interferons. Annu. Rev. Biochem. 67, 227–264.

Taniguchi, T., Takaoka, A., 2001. A weak signal for strong responses: interferon-alpha/beta revisited. Nat. Rev., Mol. Cell. Biol. 2, 378–386.

Turner, G., 1967a. Respiratory infection of mice with vaccinia virus. J. Gen. Virol. 1, 339–402.

Turner, G., 1967b. Respiratory infection of mice with vaccinia virus. J. Gen. Virol. 1, 399–402.

van den Broek, M., Muller, U., Huang, S., Aguet, M., Zinkernagel, R., 1995. Antiviral defense in mice lacking both alpha/beta and gamma interferon receptors. J. Virol. 69 (8), 4792–4796.

Verardi, P., Jones, L., Aziz, F., Ahmad, S., Yilma, T., 2001. Vaccinia virus vectors with an inactivated-interferon receptor homolog gene (B8R) are attenuated in vivo without a concomitant reduction in immunogenicity. J. Virol. 75, 11–18.

Wang, G., Li, Y., Jiang, M., 2004. Uniqueness theorems in bioluminescence tomography. Med. Phys. 31 (8), 2289–2299.

Wessely, R., Klingel, K., Knowlton, K., Kandolf, R., 2001. Cardioselective infection with coxsackievirus B3 requires intact type I interferon signaling: implications for mortality and early viral replication. Circulation 103 (5), 756–761.

Williamson, J., Reith, R., Jeffrey, L., Arrand, J., Mackett, M., 1990. Biological characterization of recombinant vaccinia viruses in mice infected by the respiratory route. J. Gen. Virol. 71, 2761–2767.

Wollenberg, A., Engler, R., 2004. Smallpox, vaccination and adverse reactions to smallpox vaccine. Curr. Opin. Allergy Clin. Immunol. 4 (4), 271–275.

Zhang, W., Feng, J., Harris, S., Contag, P., Stevenson, D., Contag, C., 2001. Rapid in vivo functional analysis of transgenes in mice using whole body imaging of luciferase expression. Transgenic Res. 5, 423–434.